International Journal of Concrete Structures and Materials
Vol.9, No.4, pp.439–451, December 2015
DOI 10.1007/s40069-015-0120-9
ISSN 1976-0485 / eISSN 2234-1315

Effects of Isolation Period Difference and Beam-Column Stiffness Ratio on the Dynamic Response of Reinforced Concrete Buildings

Young-Soo Chun[1], and Moo-Won Hur[2],*

(Received January 21, 2015, Accepted November 12, 2015, Published online December 16, 2015)

Abstract: This study analyzed the isolation effect for a 15-story reinforced concrete (RC) building with regard to changes in the beam-column stiffness ratio and the difference in the vibration period between the superstructure and an isolation layer in order to provide basic data that are needed to devise a framework for the design of isolated RC buildings. First, this analytical study proposes to design RC building frames by securing an isolation period that is at least 2.5 times longer than the natural vibration period of a superstructure and configuring a target isolation period that is 3.0 s or longer. To verify the proposed plan, shaking table tests were conducted on a scaled-down model of 15-story RC building installed with laminated rubber bearings. The experimental results indicate that the tested isolated structure, which complied with the proposed conditions, exhibited an almost constant response distribution, verifying that the behavior of the structure improved in terms of usability. The RC building's response to inter-story drift (which causes structural damage) was reduced by about one-third that of a non-isolated structure, thereby confirming that the safety of such a superstructure can be achieved through the building's improved seismic performance.

Keywords: seismic isolation, period ratio, isolation effect, shaking table test, acceleration.

1. Introduction

Isolation is a method that reduces the seismic response of a building by extending its vibration period, which is achieved by inserting a special device between the building and its foundation or into a middle story. It is an effective technology that brings about great improvement in the seismic behavior of a superstructure. This technology has been verified empirically and commercialized in countries such as Japan, China, the United States, and New Zealand, all of which have had extensive experience with earthquakes, and it has been acknowledged for its excellent results. The main targets of early isolation methods were low-story buildings and high stiffness buildings, and the outstanding and successful effects of these early methods already have been demonstrated. However, the latest architectural trends are high-story, lightweight, slender buildings, and so, isolation technology is now being developed to address these gradually increasing building trends. Although most apartment housing structures in Asian countries were built originally as slab-wall structures, recent changes include more flexible structural systems such as reinforced concrete (RC) beam-column structures and flat-plate structures that can be remodeled easily. The effects of isolation technology for such building structures have not yet been confirmed (Chun et al. 2007).

Several researchers have investigated isolated building systems. For example, Ariga et al. (2006) studied the resonant behavior of base-isolated high-rise buildings in terms of long-term ground motion, and Olsen et al. (2008) also investigated long-term building responses. Deb (2004), Dicleli and Buddaram (2007), Casciati and Hamdaoui (2008), Di Egidio and Contento (2010) also have made progress in the study of isolated building systems. Komodromos et al. (2007) and Kilar and Koren (2009) focused on seismic behavior and responses through the dynamic analyses of isolated buildings. Nonetheless, further work is needed for the practical application of an isolation device. Low to medium earthquake risk regions in Asian countries are prone to seismic hazards. Thus, for building construction in these zones, seismic base isolation can be a suitable strategy as it ensures the flexibility of the building and reduces the lateral forces in a drastic manner. Although the application of an isolator is similar all over the world, currently, proper research is lacking that could implement such a device practically. So, this concern is an urgent matter for this study.

Building codes of various countries (Japan, United States, etc.) that provide for isolation standards point out that these effects may differ according to the difference in the vibration period between the superstructure and the isolation layer, and so, many codes include relevant regulations for limitations. Feng (2007) and Feng et al. (2012) presented a comparative report of the building codes of Japan for 2000,

[1]Land and Housing Institute, Korea Land & Housing Corporation, Daejeon 305-731, Korea.
[2]Department of Architectural Engineering, Dankook University, Gyeonggi-do 448-701, Korea.
*Corresponding Author; E-mail: hmwsyh@gmail.com

China for 2001, USA IBC 2012, Italy for 2008, and Taiwan for 2002, which was updated in 2010. The important point that these reports made is that regulations for limits are different in each code. Likewise, the isolation effect is expected to differ based on how the target isolation period is configured according to the characteristics of a particular building. However, until now, no definite research records have been presented on this subject.

In response to this need, this study aims to analyze isolation effects according to the difference in the vibration period between the superstructure and the isolation layer in order to provide information about how the isolation effect changes according to the configuration of the superstructure period and the target isolation period and the characteristics of the superstructure, and to compare the isolation response of a model 15-story RC flat-plate apartment building to the seismic response of a model non-isolated building.

2. Analytical Study

2.1 Studied Building and Modeling

As suggested by Roehl (1972), in this study, the dynamic characteristics of an RC frame are defined as follows based on the fundamental vibration period (T) and the beam-column stiffness ratio (ρ) of a building. The RC frame is modeled as a single-span frame with a story height of h and span of 2 h. It is assumed that all the members of the RC building have identical cross-sections and that the distribution of the mass and stiffness for each story is constant. Figure 1 is a diagram of the study model. The major variables considered in this study and its scope are as follows:

(1) Beam-column stiffness ratio (ρ)

The beam-column stiffness ratio can be defined as shown in Eq. (1). This ratio represents the different characteristics of the frame as the value changes from 0 to ∞.

$$\rho = \sum_{beam} \frac{EI_b}{L_b} \Big/ \sum_{column} \frac{EI_c}{L_c} \tag{1}$$

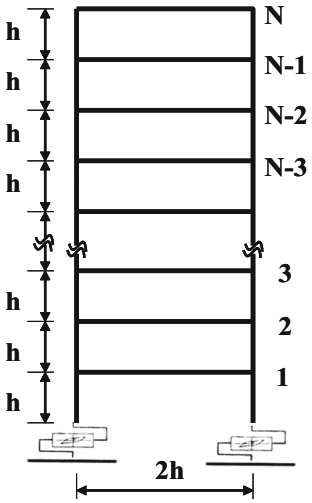

Fig. 1 Modeling for the object of study.

Here, E is the elastic modulus, I_b is the geometrical moment of the inertia of the beam, I_c is the geometrical moment of the inertia of the column, L_b is the length of the beam, and L_c is the length of the column. The value of ρ is taken from the middle story of the RC building. The limit value $\rho = 0$ represents a cantilever that consists of a beam with no restraint on its nodal rotation, and the limit value $\rho = \infty$ represents a shear building in which the nodal rotation is completely restrained. The value between the two limit values represents a frame that induces bending deflection depending on the degree of the nodal rotation in the beam and column. In this paper, the range of the ρ value is defined as between 0.05 and 2.0, which is sufficient to show the characteristics of building frames in Asia, based on existing studies. Analysis was carried out on seven values: 0.05, 0.1, 0.15, 0.2, 0.5, 1.0 and 2.0.

(2) Fundamental vibration period of building (T_1)

The fundamental vibration period of an RC building has the range shown in Eq. (2), which approximates the number of stories in the building.

$$0.6T \le T_1 \le 1.4T \tag{2}$$

Here, $T = 0.1N$ and N = number of stories in the building.

In this study, the number of stories in the RC building is 15 stories. Seven stiffness ratio models and six period models were developed with consideration of the above variables and the scope of the study, thereby interpreting and analyzing a total of 42 models. For the hysteretic characteristics of the isolation device, the characteristics (bilinear model) of a hybrid-type isolation system applied to an actual isolation design were used. For seismic motion, time history analysis was performed using the most widely used earthquake data for the El Centro (1942), Taft (1952), and Hachinohe (1968) earthquakes (refer to Fig. 2). ETABS v8.48 was the program used for analysis. The modeling of the superstructure was designed as for a frame element, and Isolator1 element was used to perform local nonlinear modeling of the isolation device. Also, five percent viscous damping was assumed for the damping of the superstructure. For the isolation layer, any viscous damping other than hysteretic damping of the isolation device was not taken into account.

2.2 Analytical Results and Comments

(1) Isolation effect according to period difference between superstructure and isolation layer

Figures 3 and 4 show the distribution of the maximum response accelerations for each story according to the change in the period of the isolated RC building when $\rho = 0.05 \sim \rho = 2.0$, which are used to examine the isolation effect according to the period difference between the superstructure and the isolation layer of the isolated building. In this study, the isolation effect according to the change in the stiffness ratio between the superstructure and isolation

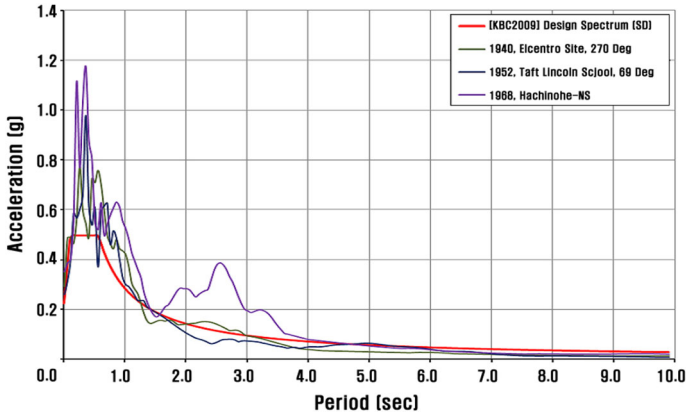

Fig. 2 Scaled response spectra of earthquake data.

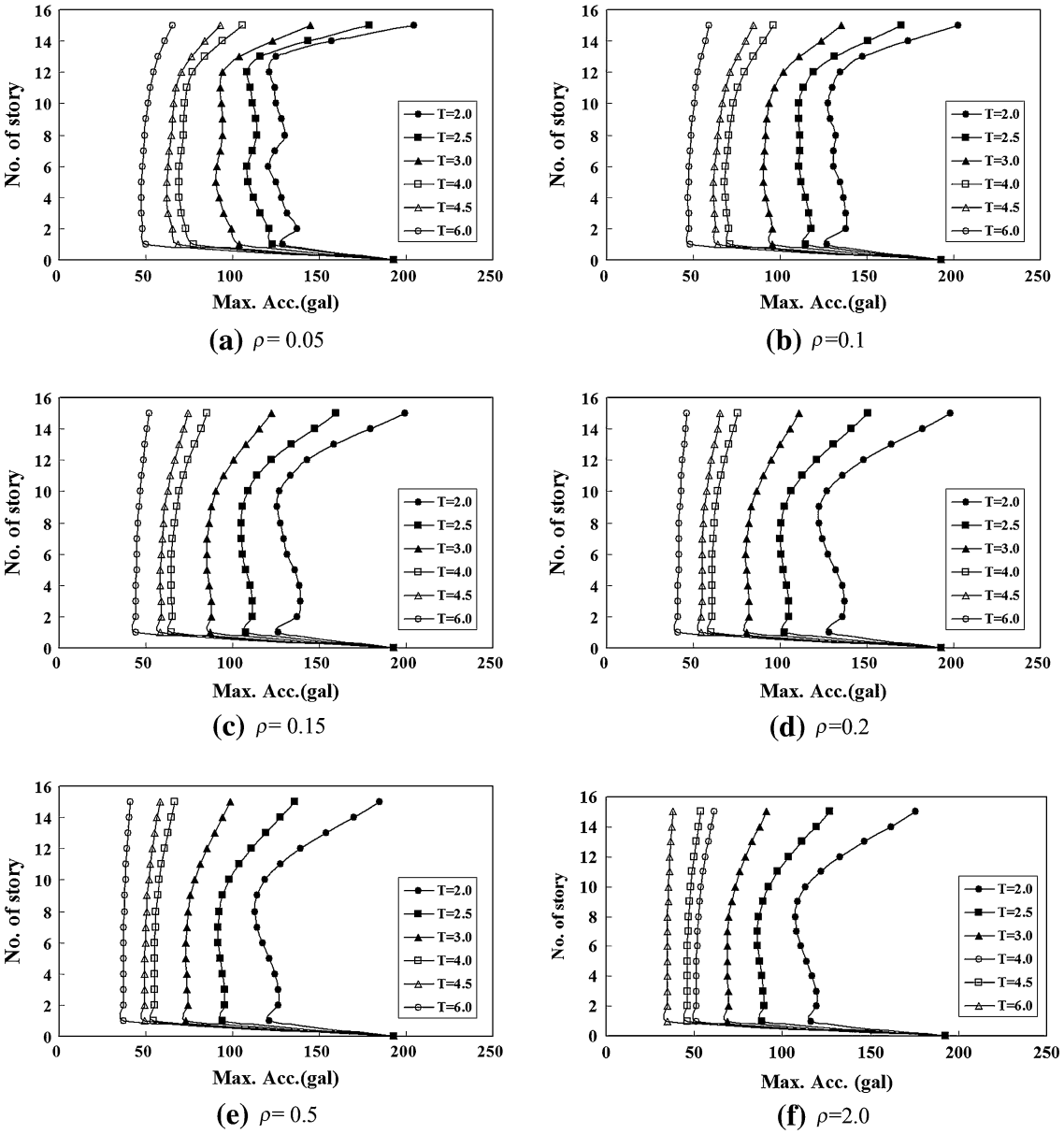

Fig. 3 Distribution of the acceleration of superstructure due to variation in period ratio.

layer was examined by changing the vibration period of the isolated building under the fixed vibration period of the superstructure.

As shown in Figs. 3 and 4, with an increase in the period of the isolated building when $\rho = 0.05 \sim \rho = 2.0$, the distribution of the response acceleration in each story of the

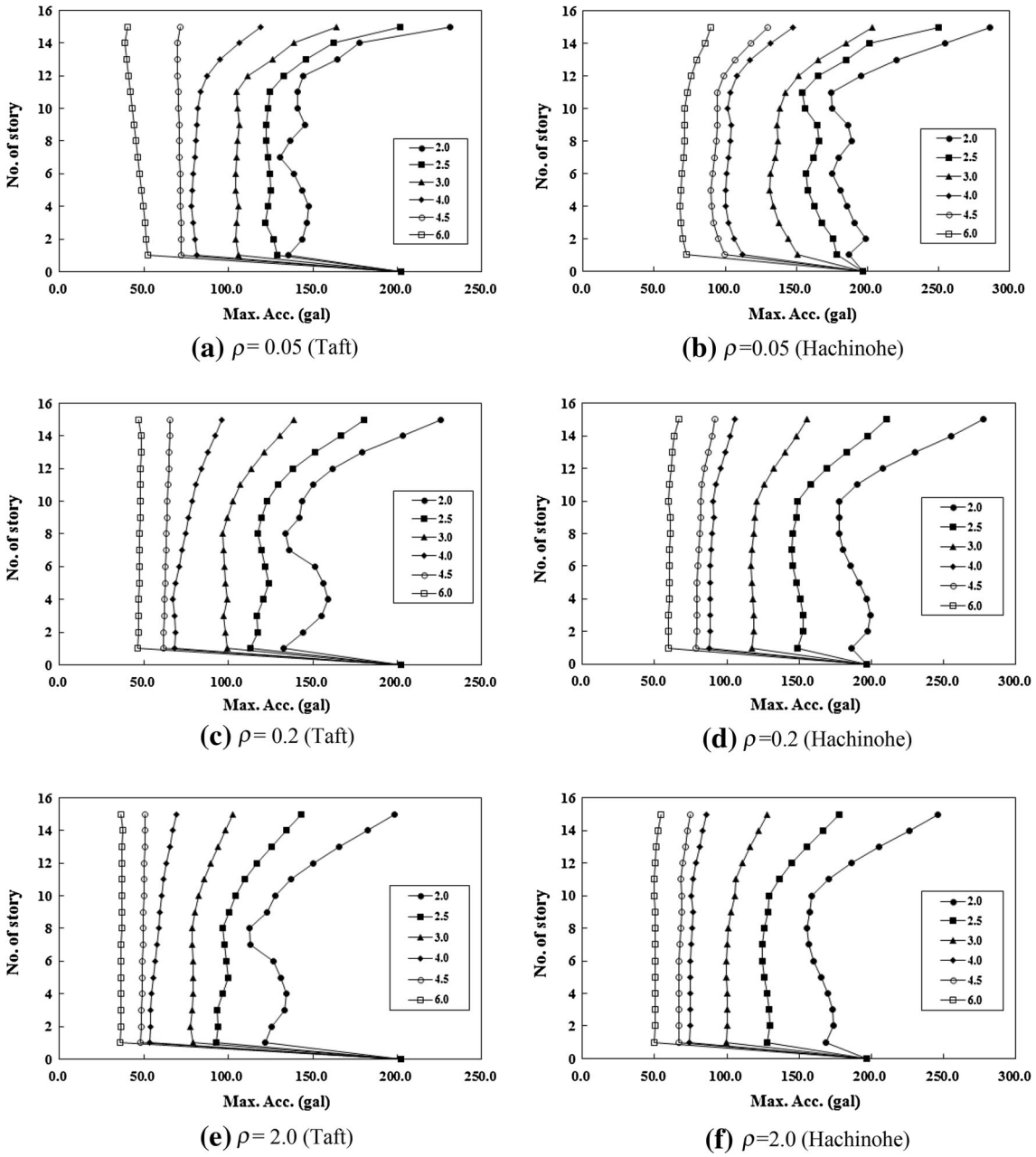

Fig. 4 Distribution of the acceleration of superstructure due to variation in period ratio (Taft and Hachinohe).

building changes from the form that includes the effect of a higher order mode to a constant distribution that is close to rigid body behavior. In terms of reduced acceleration, both buildings showed a reduction in acceleration, but it was difficult to anticipate the effective isolation, as acceleration tends to increase at the uppermost story of a building when the difference of the vibration period between the superstructure and the isolation layer is small. Considering the fact that the reduction in the acceleration of the superstructure refers to the reduced load in the member design, it is necessary to design the difference of the vibration period between the superstructure and the isolation layer to be above a certain level in order to achieve an effective isolation effect.

When the vibration period ratio between the superstructure and the isolation layer is low, the distribution of the response acceleration becomes inconsistent due to the effect of the higher order mode, which makes it difficult to achieve very much improved usability of the building. Also, a large load can act on a specific unpredicted layer to form a soft layer, which also causes difficulty in predicting the overall behavior of the RC building and assessing hazards. Because such careful design is required, it is desirable to design the model for above a certain level of the vibration period ratio between the superstructure and the isolation layer. From a practical viewpoint, it is necessary to set forth a quantitative standard for the level of the period ratio that must be achieved in order to obtain an effective isolation effect. However, no accurately established quantitative standards are currently available that can determine the isolation effect from the form of a specific response. Nevertheless, based on the comparison results shown in Figs. 3 and 4, and

considering the fact that the aim of an isolation design is to achieve a consistent response acceleration distribution in order to decrease the response acceleration and increase usability, it is recommended that the subject RC building should be designed with a isolation period that is at least 2.5 times longer than that of superstructure in order to obtain an effective isolation effect for the building.

(2) Effects according to beam-column stiffness ratio

Another interesting point that can be observed from Figs. 3 and 4 is that no large difference is evident in the responses to the beam-column stiffness ratio (ρ) of the superstructure when the period ratios of the superstructure and isolation layer are the same. This finding implies that the target isolation period does not need to be considered differently in terms of the stiffness (or the frame characteristics) of the superstructure for the isolation design. It shows that the isolation effect can be differentiated only in terms of the vibration period ratio of the superstructure and isolation layer.

3. Experimental Study

3.1 Experimental Program and Test Specimens

For the experiments in this study, an isolated RC building model and a non-isolated RC building model scaled to one-tenth of an actual building size were designed with consideration of the capacity of a shaking table. The effects of the model building foundations and site on the seismic behavior of the RC buildings were considered using seismic waves with different characteristics. The ground motion records used for the tests include those for the Central Chile earthquake S2A059 (059), San Fernando earthquake S3A103 (103), Eureka earthquake S2A105 (105), and an artificial earthquake. Earthquake 105 and the artificial earthquake represent a harmonic type of motion that is critical for long period structures. The spectrum characteristics of these seismic waves are compatible with the Korean Building Code (KBC 2009) and the US Building Code (ASCE/SEI7-10, 2010) design spectrum. The fabrication of the specimens and experimentation were carried out at the China Academy of Building Research (CABR) in Beijing, China. Figure 5 shows a typical floor plan of the subject buildings and the facade of the specimen installed on top of a shaking table. A full-scale model of the specimen, shown in Fig. 5a, is a flat-type medium sized apartment building with 15 stories and four units in each story.

The total height of the RC building is 45,800 mm including the water tank room. The plane dimensions are 50,720 mm × 12,270 mm. The story height of each story is 2800 mm, and the height of the water tank room is 1400 mm. The target isolation period of the full-scale model originally was to be configured as 4.0 s based on the criteria described in Sect. 2.2, but the isolation period was changed to 3.0 s based on the manufacturing limits of the scaled model isolation device and the effectiveness of the isolation effect. Eighteen lead rubber bearings (LRB 80) and 23 laminated rubber bearings (RB 80) were used to make the isolation layer in order to attain the target isolation period (JSSI 2006; SIVIC 2009). Table 1 presents the characteristics of each isolation device. The scaled specimen was modeled using a maximum manufacturing size that is one-tenth an actual building size to accommodate the capacity of the shaking table (6 m × 6 m, 800 KN, 6 DOF). It is a 15-story model with a long side and a short side of 5.07 m × 1.23 m respectively, and an overall height of 4.6 m. Table 2 summarizes the law of similarity for the mixed similarity model applied in this study.

3.2 Manufacture of Specimens

The concrete strength values of the full-scale model were C30 (30 MPa), C35 (35 MPa) and C40 (40 MPa), and the corresponding concrete strength values of the scaled model were M5.5 (5.5 MPa), M6.0 (6.0 MPa) and M6.5 (6.5 MPa). For the rebar, annealed fine-drawn steel bars with diameters of 0.9 ~ 2.2 mm were used based on similarity conditions. Table 3 shows the test results for the small aggregate concrete and rebar. The specimens were manufactured by first making a base-plate of reinforced concrete, then installing and curing the scaled isolation device on top of the base-plate, and creating a base-plate and superstructure for manufacture of the superstructure. The concrete placement was performed story by story, and the concrete was cured for about 3 days after placement before sequentially carrying out the construction of the upper stories.

3.3 Test Setup and Loading Procedure

Figure 6 shows a complete view of the specimen installed on top of the shaking table. After fixing the specimen to the shaking table, the insufficient additional mass was determined according to the law of similarity, as shown in Fig. 6b.

For additional artificial mass, 0.1 kN iron ingot was distributed as uniformly as possible as a single layer on top of the floor slab of each story. Seismic motion was applied sequentially in the x, y, and $x + y$ directions of the model, and the peak ground acceleration (PGA) was increased gradually to 0.07, 0.1, 0.22, 0.4 and 0.9 g. In this study, the tests were conducted with 0.22 g as the design seismic motion in order to assess the residential performance and 0.9 g as the seismic motion used to verify the safety performance. The time of the seismic motion was scaled down to the ratio of 1/4.472 for the recorded time according to the law of similarity.

The story acceleration and inter-story drift were measured to compare the capacity of the test buildings. Based on the test conditions, the story acceleration was measured every two floors, measuring four points in each direction and the center point, to find the lateral movement and warping histories of each floor, whereas the inter-story drift was measured every five floors by connecting the corners of the upper and lower sides of each floor diagonally. The ARJ-50A (Tokyo Sokki, Japan) was employed as the accelerometer, and a cable-extension displacement sensor, CDS-30 (Vishay Precision Group, Inc.), was employed as the displacement meter.

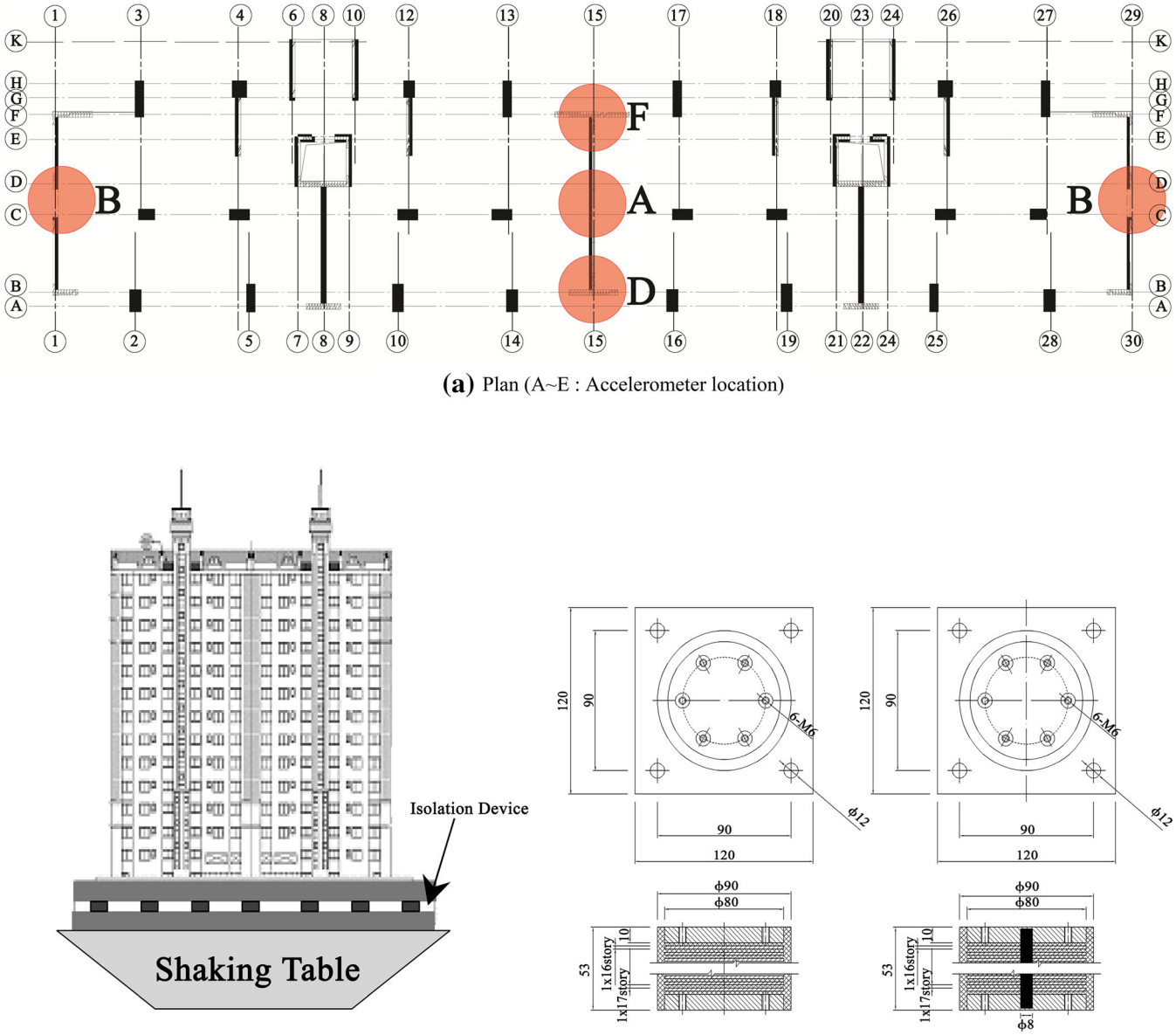

(a) Plan (A~E : Accelerometer location)

(b) Test model

(c) Isolation device (miniatures)

Fig. 5 Plan of study model, test model and isolation device.

3.4 Test Results

(1) Crack pattern and mode of failure

The isolated structure and non-isolated structure showed substantial differences in terms of scale and the type of seismic motion. First, with regard to cracking and the status of the failure, the isolated RC structure did not show any visually observed cracks in the superstructure until 0.9 g. No destructive symptom appeared until the end of the experiment. In contrast, the non-isolated RC structure was found to maintain an elastic state under small seismic loads, but cracks occurred in a portion of a structural member at under 0.22 g. Also, the structure clearly reached an inelastic state after experiencing 0.9 g, and many cracks and the destruction of some members were observed (refer to Fig. 7).

(2) Maximum drift and inter-story drift

Figure 8 shows the response to inter-story drift, which is a phenomenon that causes structural damage. In comparison to the non-isolated structure, the isolated structure shows that the almost constant response reduced by about one-third, depending on the height. Considering the fact that inter-story drift is limited as a means to determine the seismic performance of buildings, and the reduced inter-story drift in an isolated structure implies improved seismic performance, then the safety of a superstructure can be achieved. Also, Fig. 9 shows that the isolated RC structure experienced a very large drift in the isolation layer, but the maximum response drift of the isolation layer under 0.22 g was 14.76 mm, which is much lower than the allowable drift, i.e., smaller value between 0.55 d (d = diameter of isolation device) and 3 t_r

Table 1 Details of isolation devices used in 1/10-scaled model.

Group	LRB 80	RB 80
Number	18	23
Diameter × height (mm)[a]	80 × 79	80 × 79
Inner steel plate (mm)	19@1.0	16@1.0
Inner rubber plate (mm)	20@1.0	17@1.0
1st shape coefficient	17.5	17.5
2nd shape coefficient	3.5	4.12
Vertical stiffness (N/mm)	7830	3880
Effective stiffness at 50 % horizontal strain (N/mm)[b]	78	103
Damping ratio at 50 % horizontal strain[b]	0.12	0.05
Effective stiffness at 100 % horizontal strain (N/mm)[b]	62	100
Damping ratio at 100 % horizontal strain[b]	0.1	0.05
1st Stiffness (N/mm)	140	–
2nd Stiffness (N/mm)	52	–
Bucking load (N)	200	–

[a] Height: included the thickness of top and bottom plates.
[b] Effective stiffness and damping ratio in this table are average value. Difference between effective stiffness of isolation devices is no greater than ten percent.

Table 2 Scale factor of reduction model.

Quantity	Dimension	Ratio	Quantity	Dimension	Ratio
Length	L	1/10	E. Modulus	FL^{-2}	1/2.5
Stress	FL^{-2}	1/2.5	Frequency	T^{-1}	1/0.2236
Mass	FT^2L^{-1}	1/500	Time	T	1/4.472
Stiffness	FL^{-1}	1/25	Acceleration	LT^{-2}	2/1

Table 3 Test results of small aggregate concrete and characteristics of steel.

Strength	Average strength (MPa)	E. Modulus ($\times 10^4$ MPa)	Variety	Diameter	Steel no.	E. Modulus (N/mm^2)	Yield strength (N/mm^2)	Max. strength (N/mm^2)	Elongation
M5.5	7.5	1.12	14#	2.2	2#	0.8×10^5	310	400	0.26
					6#	0.8×10^5	300	400	0.30
M6.0	8.5	1.21	16#	1.6	3#	0.7×10^5	360	420	0.13
					4#	1.0×10^5	360	420	0.12
M6.5	10.0	1.40	18#	1.2	5#	0.65×10^5	360	480	0.32
					7#	0.65×10^5	300	420	0.26

(t_r = total thickness of rubber layer in isolation device), in the Chinese standard GB50011-2010 (2010) and CECS126 (2001). The maximum response drift under 0.9 g was found to be 26.46 mm, confirming that the design is appropriate for the target performance.

(3) Acceleration response

Figure 10 presents a comparison of the peak acceleration response of each story for the isolated RC structure and non-isolated RC structure. While the response acceleration of the

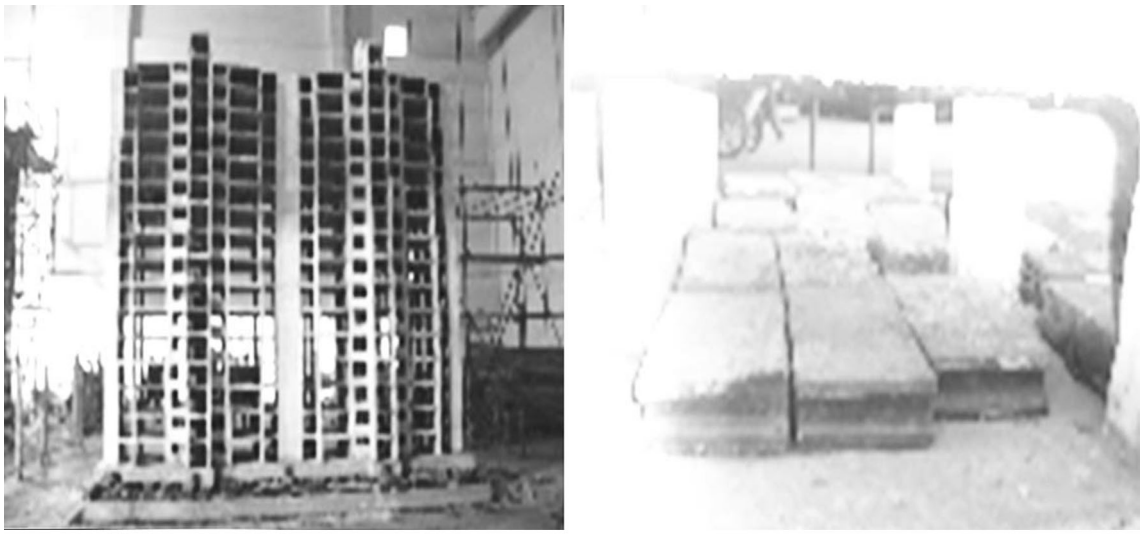

Fig. 6 Specimens and added mass setting.

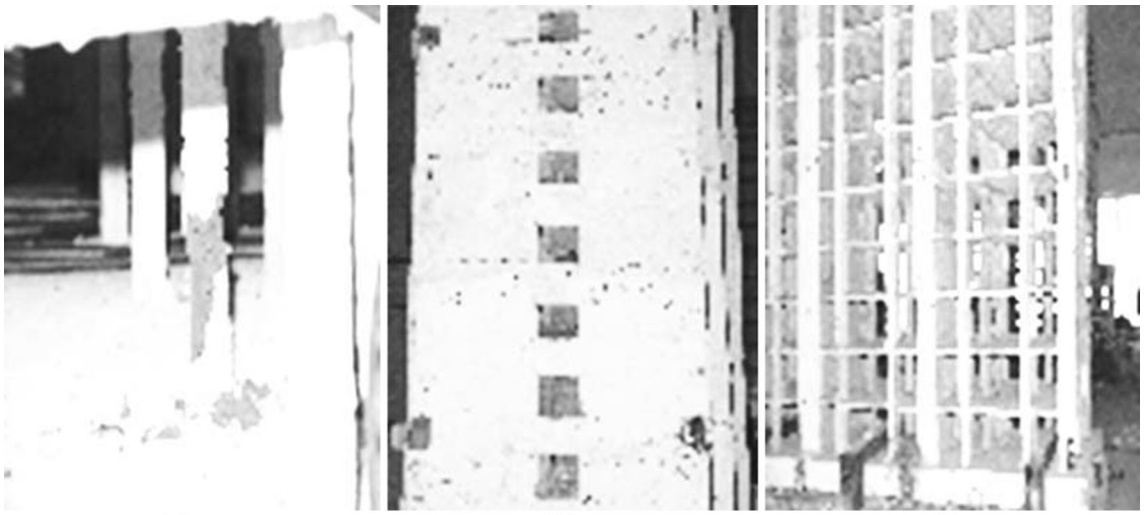

Fig. 7 Building cracks and destruction of 0.9 g.

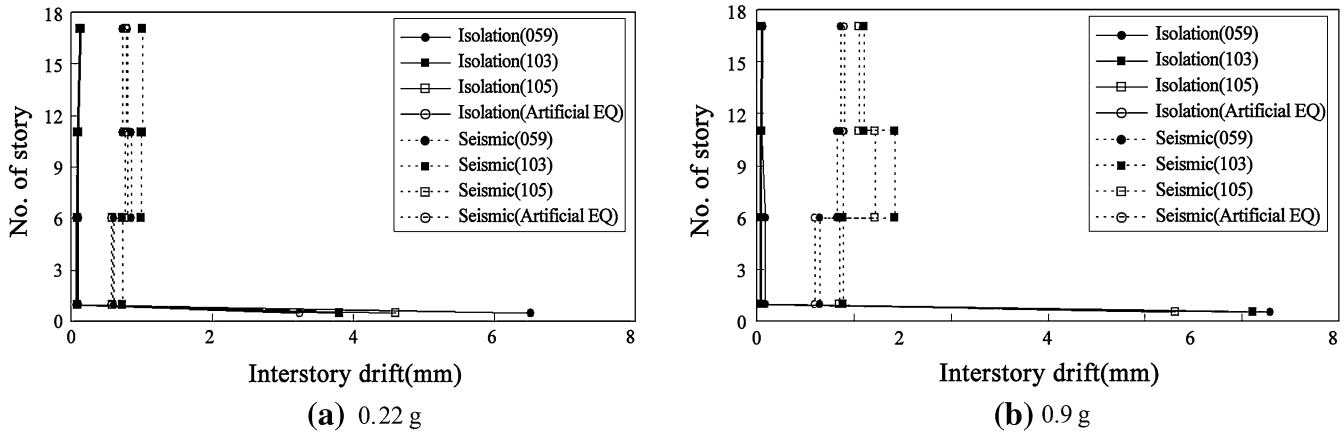

Fig. 8 Distribution of inter-story drift (Y-direction).

non-isolated structure shows a response distribution of a typical fixed-based structure in which the acceleration gradually increases as the response moves closer to the upper stories, the isolated structure shows that the almost constant response distribution and acceleration at the uppermost story is reduced by about two-thirds compared to the non-isolated structure. This improved behavior can be expected from the isolated RC structure in terms of usability, and amplification of

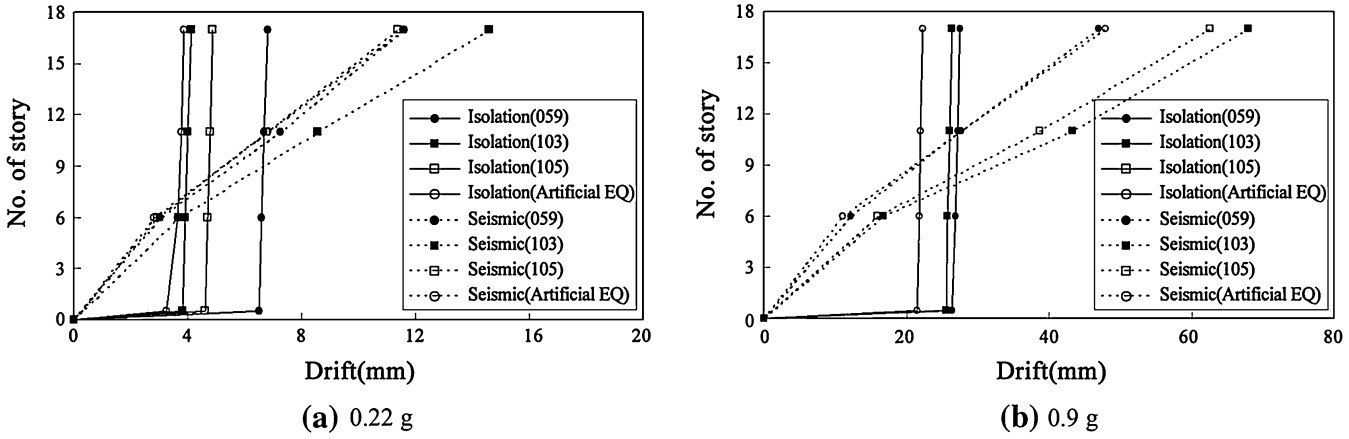

Fig. 9 Distribution of maximum drift response (Y-direction).

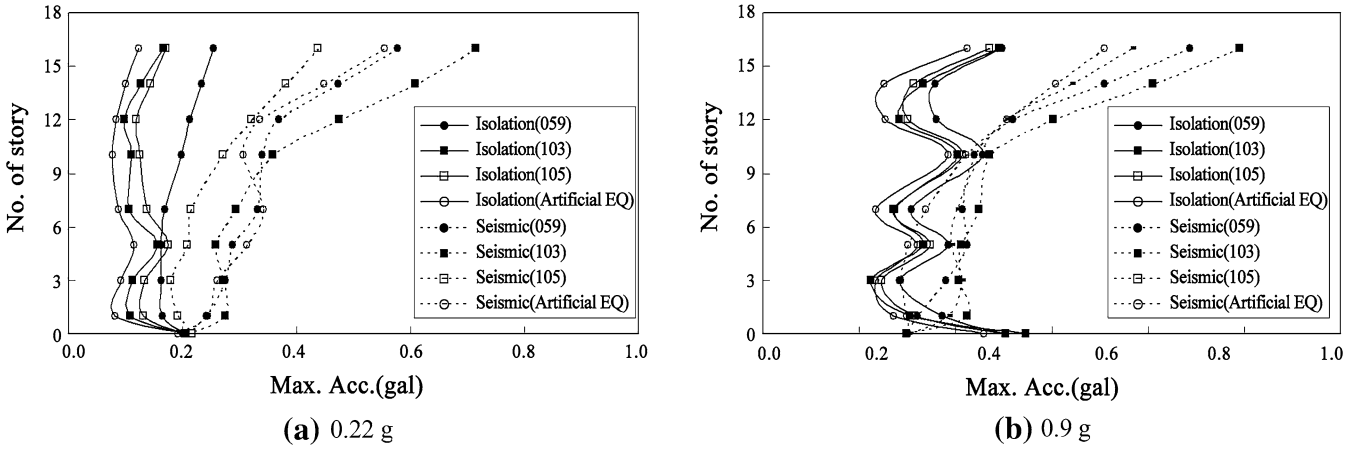

Fig. 10 Distribution of maximum response acceleration (Y-direction) on each story.

the response acceleration in the superstructure did not appear until 0.9 g. This phenomenon clearly explains the isolation effect. In addition to increased usability, greater reduction of the shear force in the superstructure can be obtained in comparison to that of the non-isolated RC structure.

However, because the period ratio between the superstructure and the isolation layer in this case did not configure as larger than 2.5 times, the distribution of the response acceleration in the isolated structure is closer to a K-shape than complete rigid body behavior. The effect of the higher order mode seems to be included, and the acceleration value did not decrease as much as the input value.

3.5 Comparison of Test Results with Response of Full-Scaled Reinforced Concrete Building

The acceleration response of the full-scale RC building could be obtained from the following relational equation with consideration of the similarity relationship presented in Table 2.

$$a_i = K_i a_g \tag{3}$$

Here, a_i is the maximum acceleration response (g) of the i story of the full-scale building, a_g is the maximum acceleration (g) of the input seismic motion, and K_i is the dynamic magnification factor of the i story of the scaled model that corresponds to the input seismic motion of a full-scaled RC structure.

Figure 11 presents a comparison of the maximum acceleration response of each story that was obtained from the test results and analytical results according to different seismic waves.

As illustrated in the figure, the experimental values are slightly higher than the values obtained from the analysis of seismic motion to assess residential performance. The figure shows an extremely large difference of about two to three times in the seismic motion values, which confirms the model's safety performance. Also, in terms of the mode shape, although the analytical results are similar to those for rigid body behavior, the experimental results include some effects of the higher order mode. The main cause of this difference is probably a technical error associated with the fabrication of the scaled model. As this problem occurred not only in the scaled model experiments but also can occur in practice, strict experimental tests and a review of the characteristics of the isolation device are essential for on-site application. The problem becomes even greater in terms

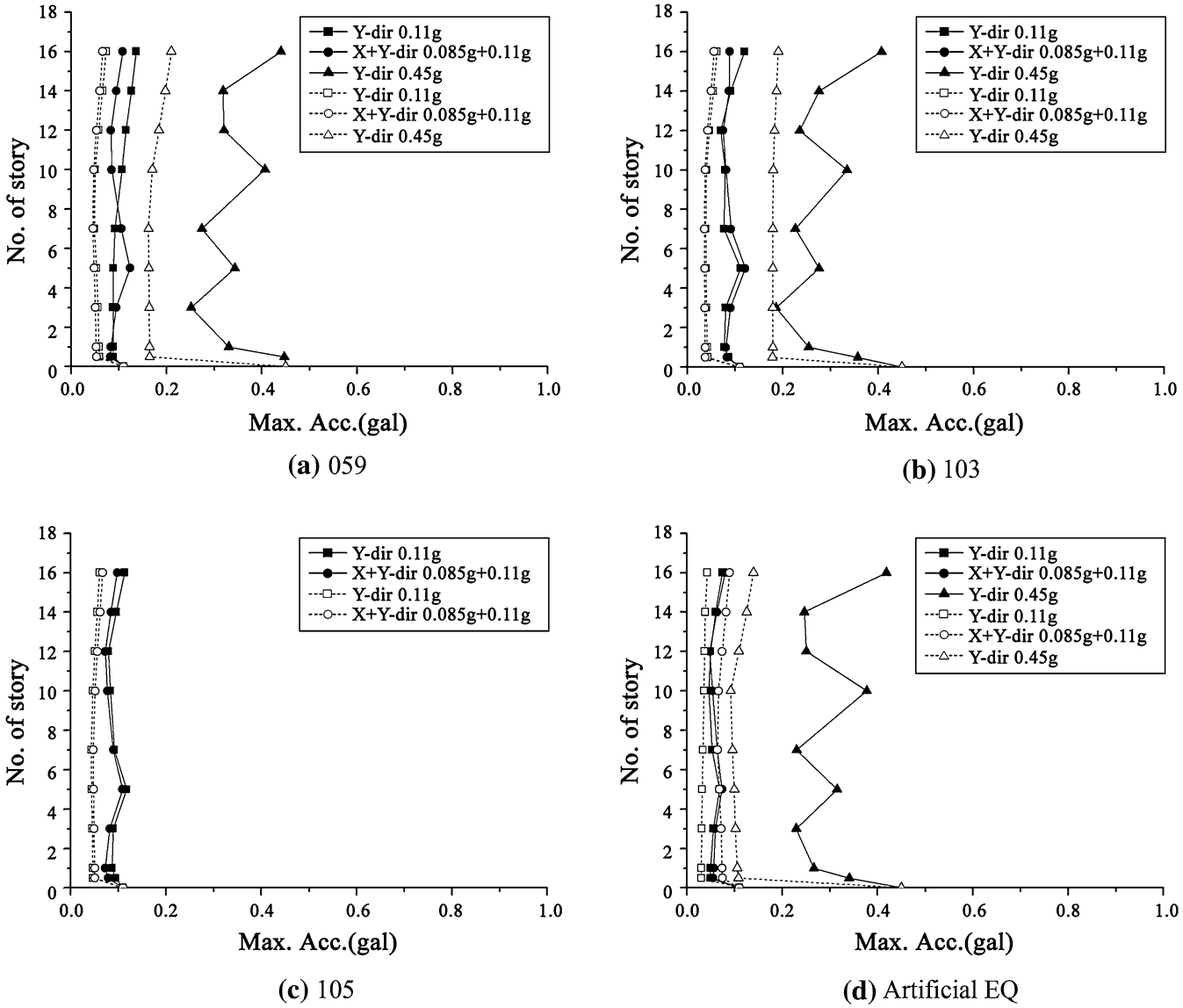

Fig. 11 Comparison of maximum acceleration response.

of the seismic motion that is used to confirm safety performance. The large difference in responses probably resulted from the large reduction in the isolation effect on the superstructure due to the smaller stiffness value difference between the superstructure and the isolation layer than the target value and from the deepening effects of the higher order mode and torsion under strong vibration due to the increased eccentricity between the superstructure and the isolation layer. However, as shown by the responses of the seismic motion that are used for the assessment of residential performance, a very similar response is evident in the one-way seismic motion, except for the slight difference in the response acceleration that is caused by the difference in stiffness value between the test results and analysis results. Based on these findings, a sufficiently reliable response can be obtained for the interpretive isolation model by paying close attention to the performance of the isolation device and appropriately modeling the stiffness of the isolation layer.

The drift response of a full-scale RC building can be obtained from the following relational equation with consideration of the similarity relationship presented in Table 2.

$$D_i = \frac{a_{mg} D_{mi}}{a_{tg} S_d} \tag{4}$$

Here, D_i is the drift response of the i story in a full-scale building (mm), D_{mi} is the drift response of the i story in the scaled model (mm), a_{mg} is the maximum input acceleration (g) of the scaled model shaking table (g), a_{tg} is the maximum input acceleration (g) of the scaled model shaking table that corresponds to D_{mi}, and S_d is the drift similarity factor of the scaled model.

Figures 12 and 13 respectively show the maximum acceleration response and maximum story displacement response that correspond to the design seismic motion level in order to assess residential performance by comparing the experimental and analytical results. As shown in the figures, the drift responses are extremely similar and constant except

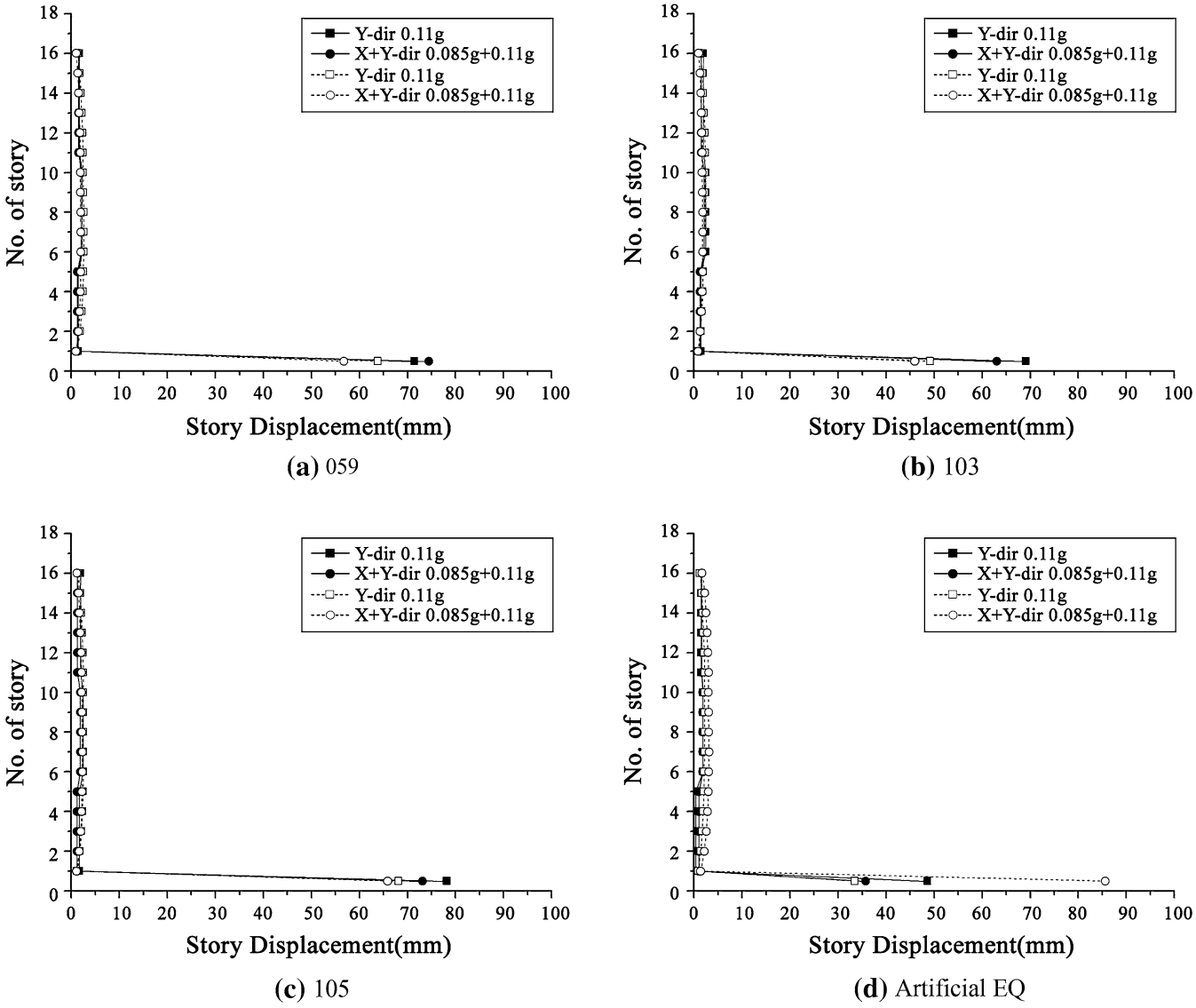

Fig. 12 Comparison of maximum acceleration response.

that the analytical results for the artificial seismic wave are slightly larger than the experimental results. The established analytical model can be used appropriately to confirm the limitation of the isolation device and to review the seismic performance of an isolated building.

4. Conclusion

In this paper, the isolation effect of a 15-story medium-rise RC building in terms of the vibration period ratio (difference in stiffness values) between a superstructure and an isolation layer and and the diverse characteristics of a frame was analyzed. Based on this analysis, the seismic behavior and performance of an isolated RC flat-plate structure were assessed by conducting shaking table tests on a model that scaled down an apartment building to one-tenth size. The conclusions of this study are as follows:

(1) In order to obtain valid seismic isolation effects for a 15-story medium-rise RC building, the isolation period must be over two and half times the fundamental vibration period of the upper structure, and the target isolation period must be more than 3 s.

(2) Based on the test results, the isolated RC structure showed that the acceleration of the uppermost story reduced by about two-thirds compared to the non-isolated RC structure. The seismic motion that is assessed to confirm the safety performance decreased by over two-thirds. Thus, a RC flat-plate structure can achieve excellent seismic performance through isolation.

(3) In terms of the inter-story drift response that causes structural damage, the response of the isolated structure decreased by about one-third compared to the non-isolated structure. This decrease in the inter-story drift can also help to achieve the safety of a superstructure.

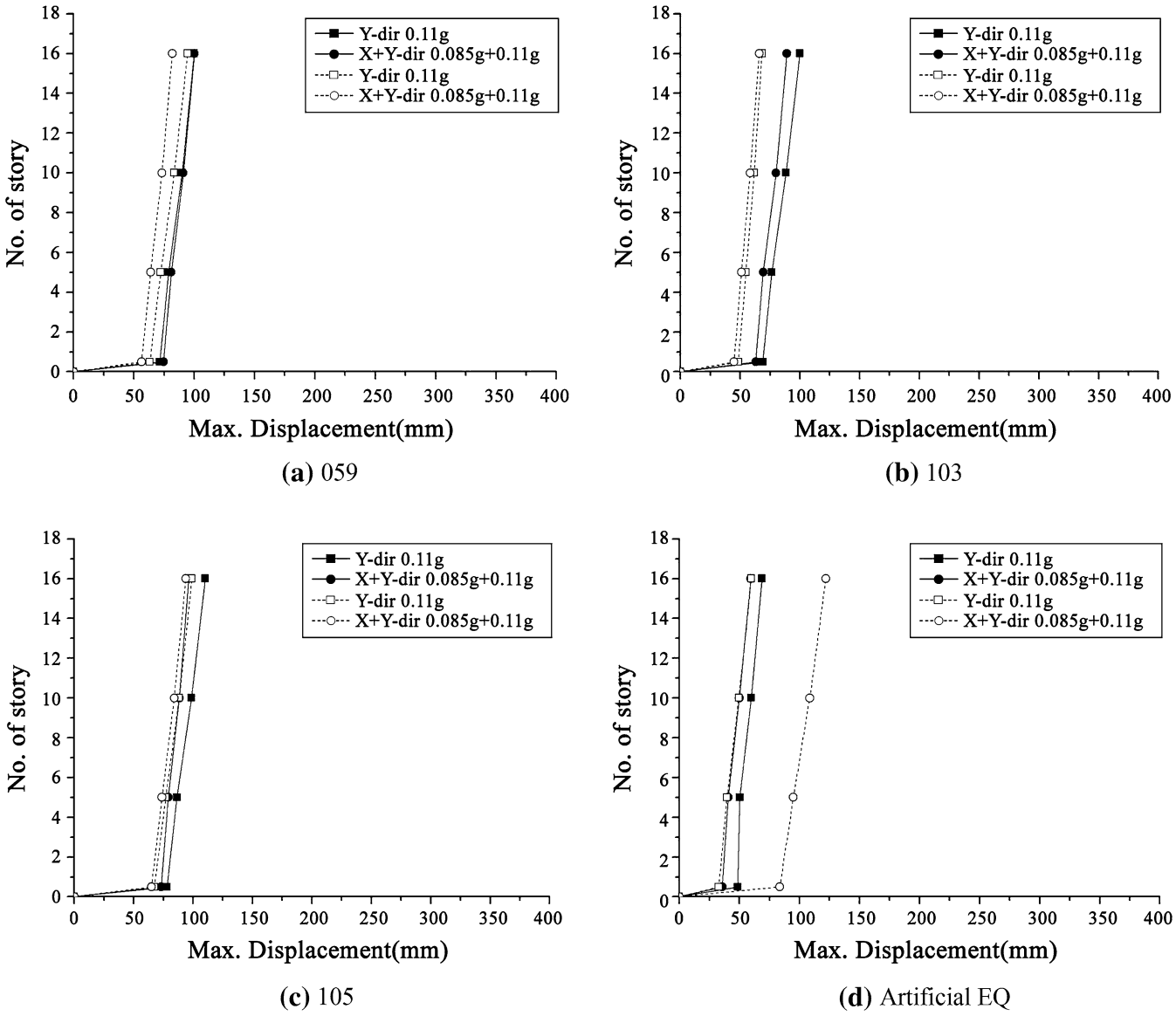

Fig. 13 Comparison of maximum displacement response.

(4) By comparing the experimental response acceleration with the analytical values, very similar responses were obtained for one-way seismic motion, except for a slight difference between the experimental results and the analysis results that was caused by the difference in stiffness value. Thus, the analytical isolation model can obtain sufficiently reliable responses through the careful confirmation of the performance of the isolation device and appropriate modeling of the stiffness in the isolation layer.

(5) As a part of the methodology to achieve effective seismic isolation behavior for a medium-rise RC building, this study presents ways to set the isolation period against the period of the upper structure and the beam-column stiffness ratio through a limited analytical study and tests on a fifteen-story reinforced concrete building. However, seismic isolation behavior is affected by a variety of variables, such as seismic waves, ground conditions, and the damping ratio, so additional research is needed to investigate these additional factors.

Acknowledgments

This research was supported by the Research Program funded by the Land and Housing Institute. Also, the China Academy of Building Research (CABR) in Beijing, China, contributed to the success of the tests and provided helpful advice. This support is gratefully acknowledged.

Open Access

References

American Society of Civil Engineers (ASCE). (2010). Minimum design loads for buildings and other structures. ASCE/SEI 7-10.

Architectural Institute of Korea. (2009). Korean Building Code and Commentary (KBC) (in Korean).

Ariga, T., Kanno, Y., & Takewaki, I. (2006). Resonant behaviour of base isolated high-rise buildings under long-period ground motions. *Structural Design Tall Special Buildings, 15*, 325–338.

Casciati, F., & Hamdaoui, K. (2008). Modelling the uncertainty in the response of a base isolator. *Probabilistic Engineering Mechanics, 23*, 427–437.

China Association for Engineering Construction Standardization. (2001). Technical specification for seismic-isolation with laminated rubber bearing isolators. CECS126 (in Chinese).

Chun, Y. S., Son, C. H., Joo, I. D., Ahn, K. S., Kim, J. P., & Choi, K. Y. (2007). Development of flat plate structure with base isolation system and analysis of economical efficiency. Research Report of Housing & Urban Research Institute, pp. 30–36.

Deb, S. K. (2004). Seismic base isolation-an overview. *Current Science, 87*(10), 1426–1430.

Di Egidio, A., & Contento, A. (2010). Seismic response of a non-symmetric rigid block on a constrained oscillating base. *Engineering Structures, 32*, 3028–3039.

Dicleli, M., & Buddaram, S. (2007). Comprehensive evaluation of equivalent linear analysis method for seismic-isolated structures represented by SDOF systems. *Engineering Structures, 29*, 1653–1663.

Feng, D. (2007). A comparative study of seismic isolation codes worldwide. *Proceedings of SIViC international seminar* (pp. 1–28).

Feng, D., et al. (2012). A new design procedure for seismically isolated buildings based on seismic isolation codes worldwide. *Proceedings of 15WCEE*: Paper No. 0435. Lisbon, Portugal.

Japan Society of Seismic Isolation (JSSI). (2006). Response control and seismic isolation of buildings. Tokyo, Japan: JSSI (in Japanese).

Kilar, V., & Koren, D. (2009). Seismic behaviour of asymmetric base isolated structures with various distributions of isolators. *Engineering Structures, 31*, 910–921.

Komodromos, P., Polycarpou, P., Papaloizou, L., & Phocas, M. (2007). Response of seismically isolated buildings considering poundings. *Earthquake Engineering and Structural Dynamics, 36*, 1605–1622.

Korea Society of Seismic Isolation and Vibration Control (SIVIC). (2009). Isolation design manual and collection of practical examples. Technical Report. Seoul, Korea (in Korean).

Ministry of Construction, P. R. China. (2010). Code for Seismic Design of Buildings. GB50011-2010 (in Chinese).

Olsen, A., Aagaard, B., & Heaton, T. (2008). Long-period building response to earthquakes in the San Francisco Bay area. *Bulletin of the Seismological Society of America, 98*(2), 1047–1065.

Roehl, J. L. (1972). *Dynamic response of ground-excited building frames*. Houston, TX: Rice University.